

Electrical and Optical Properties of Controlled Reduced Graphene Oxide Prepared by a Green and Facile Route [†]

Parsa Hooshyar ¹, Atieh Zamani ^{1,2,*}, Deniz Rezapour Kiani ¹, Shayan Fakhraeelfabadi ¹
and Mehdi Fardmanesh ^{1,*}

- ¹ SERL, Electrical Engineering Department, Sharif University of Technology, Tehran 14588-89694, Iran; parsahooshyar77@yahoo.com (P.H.); denizrezapur@gmail.com (D.R.K.); shayan.fakhraee@gmail.com (S.F.)
² Department of Converging Technologies, Khatam University, Tehran 19916-33357, Iran
* Correspondence: fardmanesh@sharif.edu (A.Z.); atieh.zamani.mail@gmail.com (M.F.)
[†] Presented at the 10th International Electronic Conference on Sensors and Applications (ECSA-10), 15–30 November 2023; Available online: <https://ecsa-10.sciforum.net/>.

Abstract: Three distinct homogeneous multilayer self-standing thin films, composed of stacked reduced graphene oxide (rGO) planes, were produced by improved Hummer's method. In order to investigate their structural, electrical, and optical properties, the samples were characterized by Raman spectroscopy, field emission scanning electron microscopy (FESEM), four-point probe measurements, and Fourier-transform infrared spectroscopy (FTIR). The Raman spectra of the samples indicate the presence of minor surface defects and a relatively low oxygen content of rGOs. The FESEM images obtained from the samples reveals a smooth sheet-like surface with few wrinkles. Additionally, the cross-sectional images provide confirmation of the presence of multi-stacked layer structures. Based on the resistance decreasing by about 0.35 to 0.65 percent per kelvin within the region of ambient temperature, the electrical resistance vs. temperature curves imply semiconducting behavior in the rGOs. The FTIR analysis of the samples conducted within the wavelength range of 2.5 to 25 μm , demonstrates a significant absorption value exceeding 90%. This observation shows that the developed materials possess favorable characteristics making them an excellent absorber candidate as for sensing detectors in the infrared range. We systematically analyzed and confirmed that the structural as well as optical and electrical properties of our obtained rGOs, may be fine-tuned by adjusting the initial reactants concentration and annealing temperature.

Citation: Hooshyar, P.; Zamani, A.; Kiani, D.R.; Fakhraeelfabadi, S.; Fardmanesh, M. Electrical and Optical Properties of Controlled Reduced Graphene Oxide Prepared by a Green and Facile Route. **2023**, *56*, x. <https://doi.org/10.3390/xxxxx>

Academic Editor(s): Name

Published: 15 November 2023



Copyright: © 2023 by the authors. Submitted for possible open access publication under the terms and conditions of the Creative Commons Attribution (CC BY) license (<https://creativecommons.org/licenses/by/4.0/>).

Keywords: graphene; spectrally wide absorber; free-standing films; thermal stability; electrical conductivity

1. Introduction

Since the emergence of graphene in 2004, numerous studies have been conducted on graphene and its derivatives, due to their remarkable properties. As a monolayer of carbon atoms held together by sp^2 covalent bonds in a honeycomb-resembling lattice, graphene was first extracted from graphite by Geim and Novoselov [1,2]. Graphene oxide (GO) and reduced-graphene oxide (rGO) are considered as the two main derivatives of graphene. GO, the oxidized form of graphene, comprises a variety of oxygen-containing functional groups, including hydroxyl and carboxyl moieties. Meanwhile, rGO is produced through the reduction process of GO, resulting in fewer oxygen-containing groups [3]. Additionally, when arranged in a stacked configuration, they would form many other derivatives including monolayer, few-layer, and multilayer graphene-based materials, each exhibiting distinct characteristics and properties [4].

Graphene and its derivatives possess distinctive characteristics that render them promising subjects for research across different applications. For instance, graphene has

high electron mobility, high electrical conductivity, high thermal conductivity, and high optical transparency [2,5–7]. These distinct characteristics make graphene-based materials appropriate for an extensive range of applications. For instance, graphene is utilized in a variety of thermal, optical, and electrical systems, such as temperature sensors [8,9], transparent electrodes [10], conductive composites (electrically, thermally, or both) [11–13], solar cells [14], and thermal imaging [15].

Most graphene synthesis methods involve the utilization of complex and costly techniques, as well as the need for three-dimensional crystal, posing difficulties for its operation and investigation [16]. On the other hand, free-standing samples offer more flexibility and versatility. In this regard, we have developed a green and facile route towards the synthesis of free-standing rGO samples. This eco-friendly route is based on the modified Hummer's method, which uses the least possible chemicals. In addition to structural analyses, the obtained samples were subjected to electrical and optical examinations to ascertain their distinct features. The interesting properties of these samples, along with their low chemical content, make them a great candidate for many applications, including medical uses such as biomedical imaging, contrast agents, and monitoring electrodes [17,18].

2. Materials and Methods

2.1. Materials

Aqueous GO solution has been initially prepared by a modified Hummers method. Pre-treatment of graphite powder favored a lower amount of reactants during synthesis. Also, the reaction time was prolonged to 34 h, which provides a good GO exfoliation without compromising the quality of the dispersion [19–22]. The concentration of the solution was 12 mg/mL, which was then air dried overnight. This was followed by thermal reduction processes to obtain rGO free-standing layers [23]. This provides an eco-friendly, safer yet a facile rGO synthesis and oxygen reduction route, which also enables mass production.

We produced three distinct rGO samples, designated *rGO1*, *rGO2*, and *rGO3*, using the described method. Notably, this approach makes no use of any mechanical or shear force. Finally, it should be mentioned that these three rGO samples were fine-tuned by adjusting the initial reactant concentration and annealing temperature. In this work, the following chemical species were used: graphite flakes (99.0%, Acros Organics), sodium nitrate (84.99, R&M Chemicals), sulphuric acid (98.0%, Sigma-Aldrich), potassium permanganate (99.0%, Sigma Aldrich), and hydrogen peroxide (27% *w/w*, Alfa Aesar) are used in this study.

2.2. Methods

The experimental approaches used in this work necessitated the use of specialized instruments to perform the relevant measurements. The Field-Emission Scanning Electron Microscope (FESEM) images of the samples were carried out using a *TESCAN MIRA 3 LMU*. A four-point probe technique was used to conduct electrical measurements. The four-point probe measurement was performed utilizing a *KEITHLEY 6221* current source (with sub pico ampere resolution) and a *KEITHLEY 2182A NANOVOTMETER*. Finally, The Fourier Transform Infrared (FTIR) spectra of the samples were obtained using Bruker's *VERTEX 70 FT-IR* Spectrometer for the purpose of analyzing their optical absorption values.

3. Results and Discussion

3.1. Structural Properties

Finding a sample's structural properties is always the initial step in learning about its properties. In order to accomplish this, our samples were initially analyzed by FESEM and Raman spectroscopy, two powerful techniques in the field of material characterization. FESEM facilitates the acquisition of high-resolution images, allowing for the detailed

examination of the morphology and structural characteristics of diverse materials at the nanoscale level [24]. The images of the rGO samples obtained through FESEM are presented in Figure 1. The multi-stacked layer architectures of these free-standing thin films are immediately apparent from these cross-sectional views. Each stacked layer is about between 2 μm to 3 μm thick and is made up of multiple rGO planes. Moreover, while looking at the surface morphology of the samples, it can be seen that they have a relatively smooth sheet-like surface with few wrinkles.

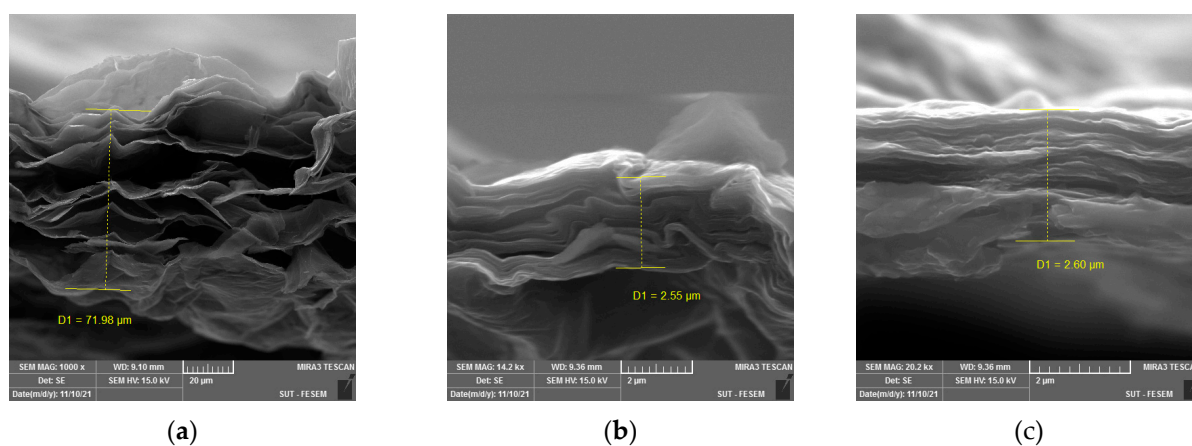


Figure 1. FESEM images of (a) rGO1, (b) rGO2, and (c) rGO3.

Raman spectroscopy complements the capabilities of FESEM by providing information on chemical structures and physical forms. Based on Raman effect and by irradiating a sample with monochromatic light and measuring the scattered light has revealed that all materials derived from graphene exhibit a G peak in their Raman spectra, which corresponds to the first-order scattering of the E_{2g} mode. Additionally, when examining oxidized derivatives of graphene, such as GO and rGO, a D band is also detected. The presence of this D band signifies a decrease in the size of the in-plane sp² domains due to the process of oxidation [25,26]. The Raman spectra obtained from our rGO samples confirm these findings and also disclose a shift of the G bands towards lower wavenumbers when compared to the G bands of the GO, which is indicative of a lower oxygen content in the rGOs. In addition, the intensity ratio between the D band and the G band (I_D/I_G) shows that the number of surface defects is small [27].

3.2. Electrical Properties

To evaluate the electrical properties of the rGO samples, we first conducted resistance measurements using the four-point probe technique at room temperature. The samples were tested in various directions to ensure comprehensive analysis. Additionally, the measurements were performed on different days to assess the stability of the samples under varying conditions. The recorded measurements demonstrate a remarkable homogeneity, as the resistance values for each sample differ only slightly across different directions.

Upon analyzing the data, we found that rGO1 exhibited an average resistance of approximately 19.38 Ω , with a deviation of $\pm 1.6 \Omega$, representing a variation of about $\pm 8.2\%$ from the average. For rGO2, the average resistance was approximately 294.25 Ω , with a deviation of $\pm 12 \Omega$, corresponding to a variation of around $\pm 4.1\%$ from the average. Finally, rGO3 displayed an average resistance of 5849.7 Ω , with a deviation of $\pm 9.5 \Omega$, indicating a variation of less than $\pm 0.2\%$ from the average. These minimal variations in resistance values, ranging from 0.2% to 8.2%, across different directions and measurements conducted on various days, are indicative of the low degree of uncertainty associated with our measurements. The consistent and stable resistance values obtained underscore the environmental and thermal stability of the samples.

According to this result, *rGO1* has the highest conductivity and is interpreted to be the most oxygen reduced sample, while *rGO3* has high resistivity and behaves the least like conductors. These results indicate that rGO samples can be produced with any desired conductivity. This brings us the versatility and tunability to synthesize rGO samples that have distinct resistances over a broad spectrum of electrical conductivity by modifying the fabrication steps. These samples were also analyzed by AC measurements and no phase change was observed between voltage and current passing through them. As a result, these free-standing homogeneous thin-films are laterally pure-resistive.

Given the potential applications of graphene-based materials as electrothermal devices, it becomes imperative to exert precise control over the impact of the temperature on electrical parameters, specifically their resistivity [28]. To acquire the electrical resistance versus temperature (RT) curves for the samples at temperatures exceeding the room temperature, we progressively increased their temperature with a heater while simultaneously monitoring their resistance. These curves are presented in Figure 2, where all the resistance values have been normalized to each sample resistance value at 300 K. With an increase in temperature, the resistance of *rGO1*, *rGO2*, and *rGO3* decreases at a rate of 0.35, 0.55, and 0.65 percent per Kelvin, in turn, implying semiconducting behavior in the rGOs. It is worth noting that the sample with higher conductivity and therefore higher reduction degree, suggesting a lower carbon to oxygen ratio, has a lower temperature coefficient of resistance (TCR), implying a decrease in its semiconducting energy gap [29].

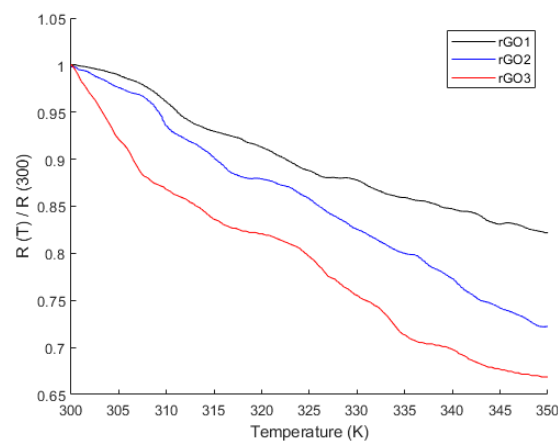


Figure 2. Resistance versus Temperature curves of *rGO1*, *rGO2*, and *rGO3*.

3.3. Optical Properties

rGO1 and *rGO2* were measured and analyzed by FTIR spectroscopy in order to investigate their optical properties. The analysis was conducted within the wavelength range of 2.5 to 25 μm . The resulting absorbance spectra of *rGO1* and *rGO2* are shown in Figure 3, indicating that both *rGO1* and *rGO2* exhibit exceptional performance across the whole spectrum. To be more specific, for *rGO1*, the absorption value exceeds 93% at wavelengths shorter than 4 μm , and its minimum absorption, observed around 12.5 μm , remains at a remarkable value of 91%. Similarly, *rGO2* demonstrates excellent absorption, with values surpassing 91.5% before 4 μm and maintaining a minimum absorption of approximately 90% at wavelengths around 12 μm and above. These results highlight the significant absorption values of the samples exceeding 90% across the entire spectrum, indicating their potential use as spectrally wide absorbers.

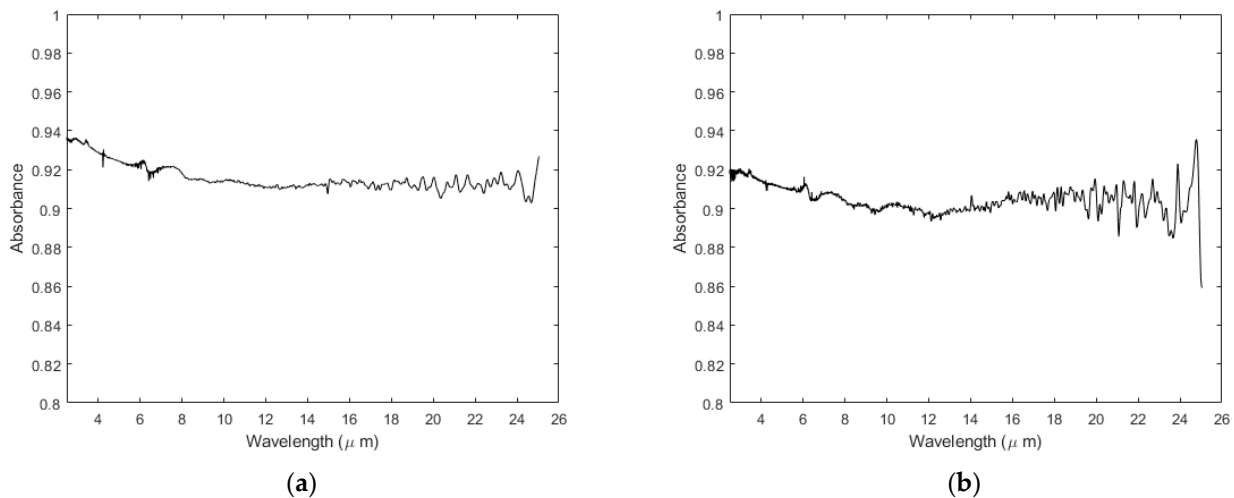


Figure 3. FTIR spectra of (a) *rGO1* and (b) *rGO2*.

4. Conclusions

The findings presented in this study provide valuable understanding into the electrical and optical properties of three multilayer rGO thin films. By using a modified version of Hummer's method, which is a facile, versatile, and environmentally friendly approach, these self-standing samples were successfully synthesized. Despite the absence of shear stress in the production process of these samples, their cross-sectional FESEM images validate the commendable attainment of a well-organized stacking arrangement. Although all samples displayed minor surface defects and a smooth sheet-like structure with few wrinkles, suggesting their high quality and uniformity, additional morphological analyses, such as Grazing-Incidence Small-Angle X-ray Scattering (GISAXS), are required to investigate the structures of the samples in more details.

According to our electrical investigations, the semiconducting behavior of the samples was evidenced by a temperature-dependent decrease in their electrical resistance, and according to the optical investigations, they showcased substantial absorption values exceeding 90% in a wide infrared range. Different electrical and optical characteristics exhibited by each sample indicate that it is possible to fine-tune the properties of rGO samples by adjusting the reactants' concentration and annealing temperature, thereby enhancing their potential for a variety of applications, including electronics, thermoelectric, and optoelectronics devices. For instance, the fact that as few chemicals as possible were used to produce the samples, coupled with their high optical absorption even in electrically conductive ranges, makes them a clean and favorable option for many biomedical applications.

Author Contributions: P.H. and A.Z. have shared the first authorship and all the authors have contributed to write and prepare the manuscript; the samples were synthesized by A.Z. and the sample preparation and measurements have been conducted by P.H., S.F. and D.R.K. under the supervision of M.F. All authors have read and agreed to the published version of the manuscript.

Funding: This research received no external funding.

Data Availability Statement: Data sharing not applicable.

Conflicts of Interest: The authors declare no conflict of interest.

References

1. Novoselov, K.S.; Geim, A.K.; Morozov, S.V.; Jiang, D.-E.; Zhang, Y.; Dubonos, S.V.; Grigorieva, I.V.; Firsov, A.A. Electric field effect in atomically thin carbon films. *Science* **2004**, *306*, 666–669.
2. Geim, A.K.; Novoselov, K.S. The rise of graphene. *Nat. Mater.* **2007**, *6*, 183–191.
3. Tahiri, M.; Del Monaco, M.; Moghanian, A.; Yarak, M.T.; Torres, R.; Yadegari, A.; Tayebi, L. Graphene and its derivatives: Opportunities and challenges in dentistry. *Mater. Sci. Eng. C* **2019**, *102*, 171–185.
4. Parvin, N.; Kumar, V.; Joo, S.W.; Park, S.-S.; Mandal, T.K. Recent Advances in the Characterized Identification of Mono-to-Multi-Layer Graphene and Its Biomedical Applications: A Review. *Electronics* **2022**, *11*, 3345.
5. Balandin, A.A.; Ghosh, S.; Bao, W.; Calizo, I.; Teweldebrhan, D.; Miao, F.; Lau, C.N. Superior thermal conductivity of single-layer graphene. *Nano Lett.* **2008**, *8*, 902–907.
6. Ghosh, S.; Calizo, I.; Teweldebrhan, D.; Pokatilov, E.P.; Nika, D.L.; Balandin, A.A.; Bao, W.; Miao, F.; Lau, C.N. Extremely high thermal conductivity of graphene: Prospects for thermal management applications in nanoelectronic circuits. *Appl. Phys. Lett.* **2008**, *92*, 151911.
7. Rokmana, A.W.; Asriani, A.; Suhendar, H.; Triyana, K.; Kusumaatmaja, A.; Santoso, I. The optical properties of thin film reduced graphene oxide/poly (3, 4 ethylenedioxythiophene): Poly (styrene sulfonate)(pedot: Pss) fabricated by spin coating. *Proc. J. Phys. Conf. Ser.* **2018**, *1011*, 012007.
8. Zeng, Y.; Li, T.; Yao, Y.; Li, T.; Hu, L.; Marconnet, A. Thermally conductive reduced graphene oxide thin films for extreme temperature sensors. *Adv. Funct. Mater.* **2019**, *29*, 1901388.
9. Liu, G.; Tan, Q.; Kou, H.; Zhang, L.; Wang, J.; Lv, W.; Dong, H.; Xiong, J. A flexible temperature sensor based on reduced graphene oxide for robot skin used in internet of things. *Sensors* **2018**, *18*, 1400.
10. Rana, K.; Singh, J.; Ahn, J.-H. A graphene-based transparent electrode for use in flexible optoelectronic devices. *J. Mater. Chem. C* **2014**, *2*, 2646–2656.
11. Kumar, P.; Yu, S.; Shahzad, F.; Hong, S.M.; Kim, Y.-H.; Koo, C.M. Ultrahigh electrically and thermally conductive self-aligned graphene/polymer composites using large-area reduced graphene oxides. *Carbon* **2016**, *101*, 120–128.
12. Yu, H.; Chen, C.; Sun, J.; Zhang, H.; Feng, Y.; Qin, M.; Feng, W. Highly thermally conductive polymer/graphene composites with rapid room-temperature self-healing capacity. *Nano-Micro Lett.* **2022**, *14*, 135.
13. Yu, S.; Li, N.; Higgins, D.; Li, D.; Li, Q.; Xu, H.; Spendelow, J.S.; Wu, G. Self-assembled reduced graphene oxide/polyacrylamide conductive composite films. *ACS Appl. Mater. Interfaces* **2014**, *6*, 19783–19790.
14. Das, S.; Sudhagar, P.; Kang, Y.S.; Choi, W. Graphene synthesis and application for solar cells. *J. Mater. Res.* **2014**, *29*, 299–319.
15. Hsu, A.L.; Herring, P.K.; Gabor, N.M.; Ha, S.; Shin, Y.C.; Song, Y.; Chin, M.; Dubey, M.; Chandrakasan, A.P.; Kong, J. Graphene-based thermopile for thermal imaging applications. *Nano Lett.* **2015**, *15*, 7211–7216.
16. Dato, A.; Radmilovic, V.; Lee, Z.; Phillips, J.; Frenklach, M. Substrate-free gas-phase synthesis of graphene sheets. *Nano Lett.* **2008**, *8*, 2012–2016.
17. Nurunnabi, M.; Parvez, K.; Nafiujjaman, M.; Revuri, V.; Khan, H.A.; Feng, X.; Lee, Y.-k. Bioapplication of graphene oxide derivatives: Drug/gene delivery, imaging, polymeric modification, toxicology, therapeutics and challenges. *RSC Adv.* **2015**, *5*, 42141–42161.
18. Cui, T.-R.; Li, D.; Huang, X.-R.; Yan, A.-Z.; Dong, Y.; Xu, J.-D.; Guo, Y.-Z.; Wang, Y.; Chen, Z.-K.; Shao, W.-C. Graphene-based flexible electrode for electrocardiogram signal monitoring. *Appl. Sci.* **2022**, *12*, 4526.
19. Paulchamy, B.; Arthi, G.; Lignesh, B. A simple approach to stepwise synthesis of graphene oxide nanomaterial. *J. Nanomed. Nanotechnol.* **2015**, *6*, 1.
20. Segal, M. Selling graphene by the ton. *Nat. Nanotechnol.* **2009**, *4*, 612–614.
21. Sharma, N.; Sharma, V.; Jain, Y.; Kumari, M.; Gupta, R.; Sharma, S.; Sachdev, K. Synthesis and characterization of graphene oxide (GO) and reduced graphene oxide (rGO) for gas sensing application. *Macromol. Symp.* **2017**, *376*, p. 1700006.
22. Chen, X.; Qu, Z.; Liu, Z.; Ren, G. Mechanism of oxidation of graphite to graphene oxide by the hummers method. *ACS Omega* **2022**, *7*, 23503–23510.
23. Roy Chowdhury, S.; Maiyalagan, T. CuCo₂S₄@B, N-doped reduced graphene oxide hybrid as a bifunctional electrocatalyst for oxygen reduction and evolution reactions. *ACS Omega* **2022**, *7*, 19183–19192.
24. Akhtar, K.; Khan, S.A.; Khan, S.B.; Asiri, A.M. Scanning electron microscopy: Principle and applications in nanomaterials characterization. In *Handbook of Materials Characterization*; Springer: Cham, Switzerland; 2018; pp. 113–145.
25. Smith, E.; Dent, G. Introduction, Basic Theory and Principles. In *Modern Raman Spectroscopy—A Practical Approach*; John Wiley & Sons, Ltd: Hoboken, NJ, USA, 2004; pp. 1–21. <https://doi.org/10.1002/0470011831.ch1>.
26. Stankovich, S.; Dikin, D.A.; Piner, R.D.; Kohlhaas, K.A.; Kleinhammes, A.; Jia, Y.; Wu, Y.; Nguyen, S.T.; Ruoff, R.S. Synthesis of graphene-based nanosheets via chemical reduction of exfoliated graphite oxide. *Carbon* **2007**, *45*, 1558–1565.
27. Palaniselvam, T.; Aiyappa, H.B.; Kurungot, S. An efficient oxygen reduction electrocatalyst from graphene by simultaneously generating pores and nitrogen doped active sites. *J. Mater. Chem.* **2012**, *22*, 23799–23805.

28. Sibia, S.; Bertocchi, F.; Chiodini, S.; Cristiano, F.; Ferrigno, L.; Giovinco, G.; Maffucci, A. Temperature-dependent electrical resistivity of macroscopic graphene nanoplatelet strips. *Nanotechnology* **2021**, *32*, 275701.
29. Jung, I.; Dikin, D.A.; Piner, R.D.; Ruoff, R.S. Tunable electrical conductivity of individual graphene oxide sheets reduced at “low” temperatures. *Nano Lett.* **2008**, *8*, 4283–4287.

Disclaimer/Publisher’s Note: The statements, opinions and data contained in all publications are solely those of the individual author(s) and contributor(s) and not of MDPI and/or the editor(s). MDPI and/or the editor(s) disclaim responsibility for any injury to people or property resulting from any ideas, methods, instructions or products referred to in the content.